Feedback Interactions Between Zinc and Phytoplankton in Seawater

William G. Sunda, Susan A. Huntsman

Limnology and Oceanography, Volume 37, Issue 1 (Jan., 1992), 25-40.

Stable URL:
http://links.jstor.org/sici?sici=0024-3590%28199201%2937%3A1%3C25%3AFIBZAP%3E2.0.CO%3B2-A

Limnol. Oceanogr., 37(1), 1992, 25–40

Feedback interactions between zinc and phytoplankton in seawater

William G. Sunda[1] *and Susan A. Huntsman*
National Marine Fisheries Service, Beaufort Laboratory, Beaufort, North Carolina 28516

Abstract

In Zn ion-buffered media, oceanic species (*Thalassiosira oceanica* and *Emiliania huxleyi*) grew at near-maximal rates at the lowest free Zn ion concentration ($[Zn^{2+}] = 10^{-12.3}$ M), whereas coastal species (*Thalassiosira pseudonana* and *Thalassiosira weissflogii*) were limited at $[Zn^{2+}] < 10^{-11}$ M. The ability of the oceanic species to outgrow coastal ones at low $[Zn^{2+}]$ was due almost entirely to a reduced growth requirement for cellular Zn rather than to an increased capability for uptake. All isolates exhibited similar sigmoidal relationships between cellular Zn : C ratios and $[Zn^{2+}]$ with minimal slopes at $[Zn^{2+}]$ of $10^{-10.5}$ to $\sim 10^{-9.5}$ M and increasing slopes above and below this range. The minimal slopes at intermediate $[Zn^{2+}]$ could be explained by negative feedback regulation of a high-affinity Zn uptake system, while increased slopes at high $[Zn^{2+}]$ appeared to be related to uptake by a low-affinity site. Measured relationships between cellular Zn : C ratios and $[Zn^{2+}]$ agreed well with those computed from a modified Redfield model based on depth profiles for Zn and PO_4 concentrations and Zn chelation in the nutricline of the North Pacific. This agreement provides evidence that Zn concentrations in the nutricline are controlled by biological uptake and regeneration as occurs for major nutrients.

There is mounting evidence that the distribution and chemical speciation of certain trace metal nutrients and the growth and species composition of phytoplankton communities are tightly linked (Morel and Hudson 1984; Sunda 1991). Like major nutrients, many trace metal nutrients occur at concentrations in surface oceanic waters that are orders of magnitude lower than those in coastal environments. Two of the most important metallic micronutrients, Fe and Zn, occur at 10^{-10} M or less in oceanic waters, but are present at 100–1,000 times higher concentrations in coastal and estuarine waters (Bruland and Franks 1983; Evans 1977; Martin and Gordon 1988; Martin et al. 1989). The marked neritic-oceanic differences in the concentrations of these metals are associated with large corresponding variations in the growth requirements of neritic and oceanic algal species for these micronutrients, providing evidence that both metals have had a marked influence on the evolution and spatial distribution of phytoplankton species (Brand et al. 1983).

Large increases also occur with depth in the concentrations of many trace metal nutrients and nutrient analogs resembling observed increases in major nutrient concentrations. Zn has been found to increase from 0.07 nM in surface waters of the central North Pacific to 8 nM at 1,500 m, and its concentration is linearly correlated with that of silicic acid (Bruland 1980). Concentrations of Cd, a nutrient analog for Zn (Price and Morel 1990), increase by 1,000-fold between the surface and 1,000 m at the same location, and the shape of the Cd profile closely resembles that of PO_4 (Bruland 1980). Likewise, dissolved Fe in the northeast Pacific increases from <0.1 nM near the surface to 1.0 nM in the oxygen minimum layer, and its concentration is correlated with nitrate, silicate, and phosphate concentrations (Martin and Gordon 1988; Martin et al. 1989). The close match between vertical distributions of trace metal nutrients and those of major nutrients provides indirect evidence for the biological control of trace metal concentrations as outlined in the classical Redfield model for major nutrients (Redfield et al. 1963), but direct evidence for this control is lacking.

One major obstacle in applying Redfield models to trace metal nutrients is the difficulty in relating measured metal concen-

[1] Present address: Office of Naval Research, Code 1123C, Arlington, Virginia 22217-5000. Reprint requests should be sent to the Beaufort Laboratory.

Acknowledgments

This work was partially funded by a grant from the Office of Naval Research.

We thank Kenneth Bruland, Larry Brand, François Morel, and an anonymous referee for reviews of this manuscript.

trations in seawater to amounts present in plankton. This difficulty results from the fact that trace metal uptake is usually controlled by the concentration of free aquated ions or of kinetically labile inorganic metal species (free ions plus inorganic complexes) (Sunda and Guillard 1976; Anderson et al. 1978; Hudson and Morel 1990) and by the fact that trace metals are complexed to varying degrees by natural organic ligands. This complexation reduces free metal ion concentrations and, therefore, metal bioavailability. Until recently there have been no data on the extent to which important micronutrient metals are complexed in seawater, and thus, no way of quantifying the extent to which complexation affects biological uptake of these metals.

For Zn, this uncertainty has been removed by recent anodic and cathodic stripping voltametric measurements of organic complexation (Bruland 1989; Donat and Bruland 1990). These measurements indicate that Zn is complexed in central North Pacific seawater by a relatively long-lived, high-affinity organic ligand whose concentration is essentially constant (1.2 nM) throughout the upper 500 m of the water column. In surface seawater, the concentration of Zn (~0.1 nM) is well below that of the ligand, and ~98% of the metal is organically complexed (Bruland 1989). At greater depths, the dissolved Zn concentration exceeds that of the ligand, and organic complexation is relatively unimportant. The combination of increasing Zn concentration and decreasing extent of organic complexation results in a 1,000-fold increase in free Zn ion concentration between the surface and depths below 500 m.

A final obstacle to the use of Redfield models to examine biological regulation of marine trace metal distributions is the lack of reliable data on the relationships between free metal ion concentrations in seawater and the uptake of metals by marine phytoplankton. Our ability to measure such relationships, however, has been greatly enhanced by the development of trace metal ion-buffered systems that enable the regulation and quantification of free ionic trace metals in culture media over wide ranges of concentrations. These buffers have been used to quantify the relationships among free ion concentrations, algal uptake kinetics, cellular metal concentrations, and growth rates for several nutrient and toxic trace metals (Brand et al. 1983, 1986; Sunda and Huntsman 1983, 1986; Harrison and Morel 1983). Although experiments have been run that examine growth limitation of oceanic and coastal species as a function of free Zn ion concentration (Anderson et al. 1978; Brand et al. 1983), corresponding relationships between free Zn ion concentration and cellular Zn, and between cellular Zn and growth rate, have not been determined.

Here we describe results of radiotracer experiments in trace metal ion-buffered seawater that examine the relationships among free Zn ion concentrations, Zn transport kinetics, cellular Zn : C ratios, and growth rates for estuarine (*Thalassiosira pseudonana* and *Thalassiosira weissflogii*) and oceanic (*Thalassiosira oceanica* and *Emiliania huxleyi*) species, previously found to exhibit characteristic neritic-oceanic differences in Zn growth requirements (Anderson et al. 1978; Brand et al. 1983). These experiments had three major objectives. The first was to determine whether the differences in requirements of the isolates for external Zn were due primarily to differences in their capabilities for intracellular transport or primarily to differences in their growth requirements for cellular Zn. The second was to examine the short-term kinetics of cellular Zn uptake to determine the characteristics of the transport system and to determine if the uptake kinetics are regulated by negative feedback mechanisms, as observed previously for algal uptake of Mn (Sunda and Huntsman 1985, 1986), Fe (Harrison and Morel 1986), nitrate (Gotham and Rhee 1981*b*), and phosphate (Gotham and Rhee 1981*a*). The third objective was to use a Redfield-type model to examine the extent to which the uptake of Zn by algal cells could explain the relationships between dissolved Zn and major nutrients observed in seawater. This model was based on published vertical distributions of Zn and PO_4 concentrations in the nutricline of the North Pacific, data for Zn complexation in these waters, and Redfield ratios of PO_4 : C in ma-

rine plankton. Relationships between Zn:C molar ratios in plankton and free Zn ion concentrations computed from the model were compared with relationships between these parameters measured in phytoplankton cultures to test the validity of the model.

Materials and methods

Experiments were run with two estuarine diatoms, *T. pseudonana* (clone 3H) and *T. weissflogii* (clone VA59), isolated from Moriches Bay, Long Island, and Chesapeake Bay, respectively; an oceanic diatom, *T. oceanica* (clone 13-1), isolated from the Sargasso Sea; and two clones of an oceanic coccolithophore, *E. huxleyi* (BT6 and A1383), isolated respectively from the Sargasso Sea and Gulf of Mexico. Axenic cultures of clones 3H, BT6, and 13-1 were obtained from R. R. L. Guillard (Bigelow Laboratory). Clones A1383 and VA59 were obtained from L. Brand (U. Miami) and the culture collection of Virginia Institute of Marine Sciences, respectively. The cultures were kept in f/2 medium (Guillard and Ryther 1962) by means of sterile technique until needed.

Both long-term and short-term Zn uptake experiments were conducted utilizing methods and procedures similar to those in previous radiolabel studies with Mn and Fe in clones 3H and 13-1 (Sunda and Huntsman 1983, 1985, 1986; Sunda et al. 1991). Long-term growth and Zn accumulation experiments were conducted with all of the isolates, whereas short-term uptake kinetic experiments were conducted only with clone BT6. All experiments were conducted at 20°C and pH 8.2±0.1 (±range) in 450-ml polycarbonate bottles containing 200 ml of 36‰ seawater medium. Cells were grown under fluorescent lighting (Vita-Lite; Duro Test Corp.) provided at an intensity of 600 μmol quanta m^{-2} s^{-1} on a 14:10 h L/D cycle.

Media used in experiments were prepared from natural seawater, collected from the Gulf Stream with a peristaltic pumping system (Sunda and Huntsman 1983). The water was stored in the dark for 18 months at 7°C and filtered through 0.4-μm Nuclepore filters just before use. To prepare media, we enriched the seawater with 35 μM $NaNO_3$, 1.5 μM Na_2HPO_4, 40 μM Na_2SiO_3, and 0.1 μg $liter^{-1}$ of vitamin B_{12}. The media also received additions of trace metal ion buffer systems, used to quantify and control free ion concentrations of Zn and other important trace metal nutrients.

For long-term experiments, these buffers consisted of 0.1 mM ethylenediaminetetraacetic acid (EDTA), 1 μM $FeCl_3$, 124 nM $MnCl_2$, 40 nM $CuCl_2$, 100 nM $CoCl_2$, and various additions of Zn labeled with ^{65}Zn. For short-term kinetic studies, the buffers consisted of 0.5 mM nitrilotriacetic acid (NTA), 1 μM $FeCl_3$, 6.5 nM Mn (2.5 nM $MnCl_2$ plus 4 nM ambient background concentration in the medium), 500 nM $CuCl_2$, and 10 nM $CoCl_2$. Zn was added along with an equivalent concentration of EDTA or NTA so that its addition at high concentrations would not appreciably alter the free EDTA or NTA concentration and thereby alter the free ion concentrations of other trace metals. NTA rather than EDTA was used in the short-term kinetic studies because of its much lower stability constants for complex formation and the associated faster dissociation kinetics of metal-NTA chelates. After addition of buffers, the media were equilibrated for 24 h before inoculation of cells.

For long-term experiments cells were transferred from f/2 medium to experimental medium containing no added Zn or ^{65}Zn ($\log [Zn^{2+}] = -12.3$ based on the background [Zn] of 4.6 nM). They were acclimated for 4–13 d (depending on the culture growth rate) and then inoculated into ^{65}Zn-labeled media at biomass levels of 0.1–0.2 μmol cell C $liter^{-1}$ of medium. The algae were grown for 12–13 cell generations to the end of the exponential phase. During this time, total cell concentrations and volumes were measured daily with a Coulter multichannel electronic particle counter (model TA-2). Specific growth rates of cultures were computed from linear regressions of ln cell volume vs. time for the exponential phase of growth.

The cultures were measured for cellular Zn concentrations during exponential growth (9–10 cell divisions after inoculation) by filtering the cells onto 3-μm Nuclepore filters and measuring them for ^{65}Zn

activity with an LKB CompuGamma automated gamma counter. The ^{65}Zn activity in the cells was corrected for filter blanks of media without cells. The corrected values were divided by the measured total ^{65}Zn activity added, multiplied by the total [Zn], and divided by the measured total volume of cells to give cellular Zn concentrations in units of mol Zn liter^{-1} of cell volume.

Cellular Zn concentrations were converted to cell Zn : C mole ratios by dividing them by cell C : cell volume ratios, measured in exponentially growing cultures containing $H^{14}CO_3^-$ and no ^{65}Zn. To measure cell C, the cultures were grown in the ^{14}C-labeled media for 5–10 generations, filtered onto 3-μm Nuclepore filters, fumed with concentrated HCl to remove inorganic C, and measured for particulate ^{14}C by liquid scintillation counting. ^{14}C activity in the cells was then divided by the measured total ^{14}C activity in the unfiltered culture medium, multiplied by the total inorganic C concentration (2.3 mM), and divided by the total cell volume measured by Coulter counter. The C : volume ratios were 12, 22, 22, 18, and 5.6 mol C liter^{-1} for clones 13-1, BT6, A1383, 3H, and VA59.

Short-term uptake experiments were conducted to examine the effect of acclimation to external Zn ion concentration on cellular uptake kinetics of Zn. In these experiments, cultures were grown for 8 and 11 d, respectively, in NTA metal ion-buffered media without ^{65}Zn at low (6 nM) and high (1.0 μM) total Zn concentrations. Cells from log-phase growing cultures were filtered gently onto 3-μm Nuclepore filters, washed with fresh medium without added Zn, and resuspended into experimental media containing various concentrations of Zn labeled with ^{65}Zn. To measure ^{65}Zn uptake, we filtered the cells onto Nuclepore filters at ~0.03, 0.25, 0.5, 1, 2, 4, 6, and 24 h after their addition to labeled media and washed them with fresh Gulf Stream water. The total cell volume in the uptake cultures was measured by Coulter counter at each sampling time. The concentration of Zn taken up by the cells was determined by the same methods and procedures described above for the long-term Zn uptake experiments.

Free ion concentrations of Zn and other trace metal nutrients in the media were computed from total metal concentrations and the extent of metal complexation by EDTA, NTA, and inorganic ions. Total dissolved Zn ranged from 4.6 to 1.0 mM in the EDTA-buffered media and 6.0 to 50 μM in NTA media, as computed from the sum of the concentrations of background Zn in the medium, carrier Zn added with the radiotracer solution, and that added as $ZnCl_2$. Background Zn and that in the radiotracer solution were measured by atomic absorption spectrophotometry (Sunda et al. 1990).

The extent of metal complexation in the media was computed from equilibrium calculations similar to those in previous algal studies in EDTA and NTA metal ion buffer systems (Sunda and Huntsman 1983, 1985, 1986). For Zn in EDTA media, the concentration of inorganic ions was computed with an experimentally measured conditional stability constant of 6.4×10^7 M^{-1}. This constant was defined by the equation

$$\frac{[ZnEDTA^{2-}]}{[Zn'][EDTA']} = K_c' \qquad (1)$$

where [Zn'] is the total concentration of dissolved inorganic Zn species (free Zn ions and inorganic complexes) and [EDTA'] is the concentration of EDTA complexes with Ca and Mg ions. The constant was measured in filtered 36‰ Gulf Stream water, with a Sep-Pak adsorption method (Sunda and Huntsman in prep.) similar to that previously described for Cu (Sunda and Hanson 1987). In this method, Zn adsorption onto Sep-Pak cartridges was measured with ^{65}Zn. Our measured stability constant ($10^{7.81}$ M^{-1}) is in good agreement with the value ($10^{7.9}$ M^{-1}) measured previously in seawater by differential pulse anodic and cathodic stripping voltametry (Donat and Bruland 1990).

The free Zn ion concentration in algal media was computed from the equation

$$[Zn^{2+}] = 0.66[Zn'] \qquad (2)$$

where 0.66 is the ratio of free Zn ions to total inorganic Zn species at 20°C computed from the equilibrium speciation model of Byrne et al. (1988). Overall, the calculations

yielded a ratio of free Zn ions to total dissolved Zn of $10^{-3.99}$. Free Zn ion concentration ranged from $10^{-12.3}$ to $10^{-8.9}$ M in three experiments and $10^{-12.3}$ to $10^{-6.9}$ M in two others.

Free Zn ion concentrations in the NTA-buffered media and free cupric, Mn, and Co ion concentrations in both sets of media were determined from equilibrium calculations (Sunda 1984) with stability constants taken from Martell and Smith (1974). The computed ratio of free Zn ion to total Zn concentration in the NTA-buffered media was $10^{-2.81}$. Computed free ion concentrations of Cu, Co, and Mn were $10^{-13.5}$, $10^{-10.6}$, and $10^{-8.1}$ M in the EDTA medium and $10^{-11.4}$, $10^{-10.6}$, and $10^{-8.4}$ in the NTA medium.

A Zn speciation model was constructed to determine relationships between dissolved Zn and free Zn ion concentrations in seawater. This model was based on the recent data for Zn complexation in the nutricline of a station in the central North Pacific (Bruland 1989) described above. The equation for this model was

$$\text{Dissolved Zn} = \frac{[Zn^{2+}]}{0.66} + \frac{1.2 \times 10^{-9}[Zn^{2+}]10^{11.0}}{[Zn^{2+}]10^{11.0} + 1} \quad (3)$$

where 1.2×10^{-9} M is the concentration of the conservatively distributed strong ligand that binds Zn and $10^{11.0}$ M^{-1} is the conditional stability constant for the complexation of Zn by this ligand (Bruland 1989). The value 0.66 is the ratio of free Zn ions to total dissolved inorganic Zn species described by Eq. 2.

Results

The growth rates of the neritic species (*T. pseudonana* and *T. weissflogii*) were limited at $[Zn^{2+}]$ below 10^{-11} M, while those of the oceanic isolates showed little or no limitation even at the lowest Zn ion concentration ($10^{-12.3}$ M) (Fig. 1). The ability of the oceanic algae to grow well at low $[Zn^{2+}]$ was due almost entirely to a substantial lowering of their growth requirement for cellular Zn (Fig. 2). For example, *T. oceanica* and *E. huxleyi* (clone A1383) grew at nearly maximal specific rates of 1.5 and 1.3 d^{-1} at cellular Zn : C ratios of 0.4 μmol mol^{-1} whereas *T. pseudonana* required 6–7 times this amount to achieve similar rates.

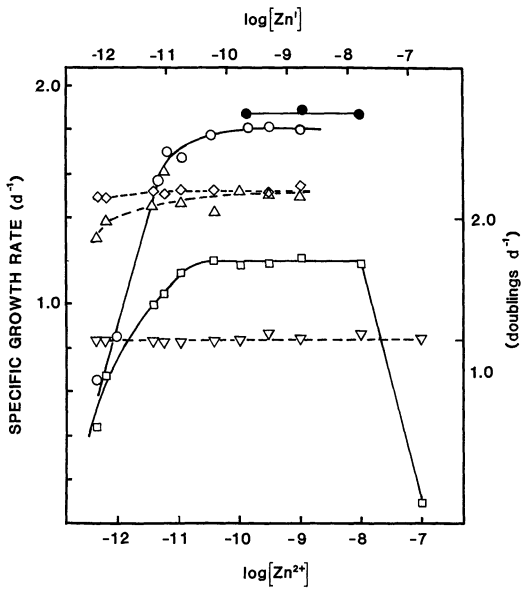

Fig. 1. Specific growth rates of coastal [*Thalassiosira weissflogii* (□) and *Thalassiosira pseudonana* (two separate experiments ○, ●)] and oceanic [*Thalassiosira oceanica* (◇) and *Emiliania huxleyi* clones A1383 (△) and BT6 (▽)] algal species as functions of $\log[Zn^{2+}]$ and log[Zn']. ($[Zn^{2+}]$ and [Zn'] are the concentrations of free Zn ions and inorganic Zn species.)

The $[Zn^{2+}]$ range was extended to 10^{-7} M in experiments with *T. weissflogii* and *E. huxleyi* (clone BT6) to examine growth and uptake response over a wider range. In these experiments, the growth rate of *T. weissflogii* was markedly inhibited at the highest Zn level, whereas that of *E. huxleyi* was unaffected (Fig. 1). The higher Zn toxicity to *T. weissflogii* was associated with a 17-fold higher cellular Zn : C ratio, suggesting that it was caused at least in part by higher Zn accumulation (Fig. 3). On the other hand, cellular Zn accumulation is proportional to uptake rate, but inversely proportional to specific growth rate (Sunda 1991), so the extremely high Zn concentration in *T. weissflogii* cells grown at $[Zn^{2+}] = 10^{-7}$ M could be caused in some measure by Zn inhibition of growth rate. Such a positive feedback situation, in which high cellular Zn accumulation inhibits growth rate and

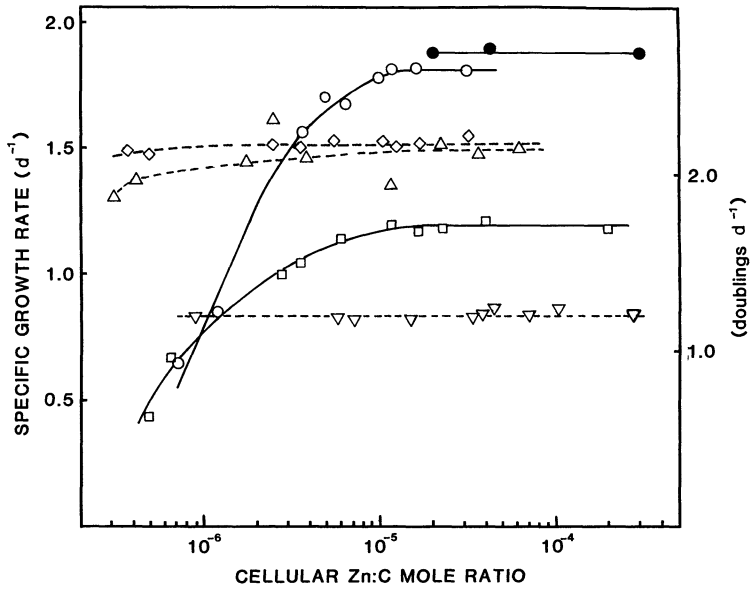

Fig. 2. As Fig. 1, but as functions of the cellular Zn : C molar ratio.

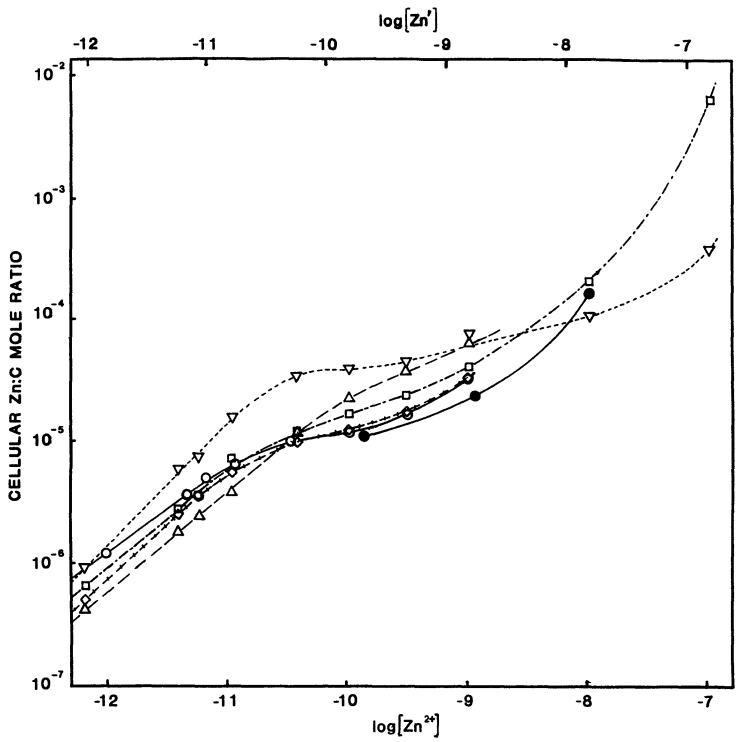

Fig. 3. Cellular Zn as functions of log[Zn^{2+}] and log[Zn']. Symbols same as Fig. 1.

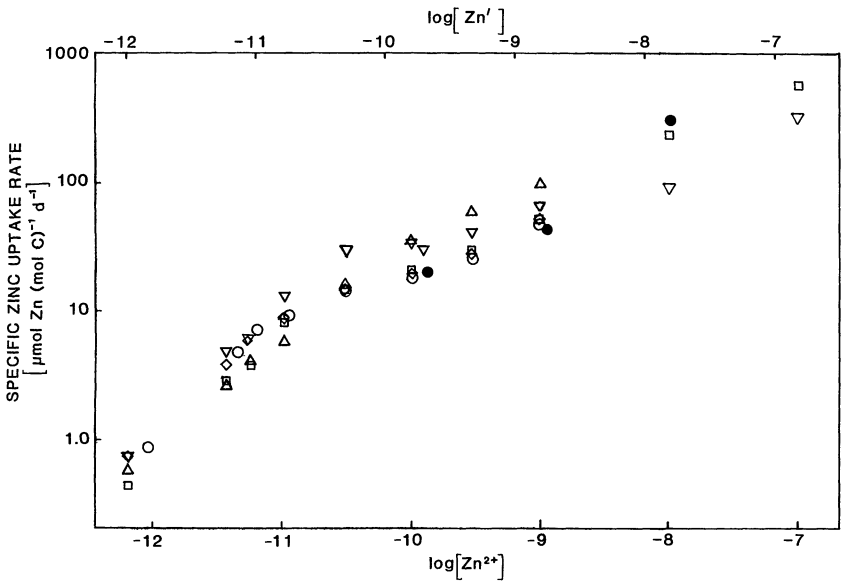

Fig. 4. Specific Zn uptake rate as functions of log[Zn^{2+}] and log[Zn']. Symbols same as Fig. 1.

decreased growth rate increases cellular Zn accumulation, could result in rather abrupt changes in both parameters, as observed for *T. weissflogii* at [Zn^{2+}] between 10^{-8} and 10^{-7} M (Figs. 1, 3).

Relationships between cellular Zn : C ratios and [Zn^{2+}] had sigmoidal shapes (Fig. 3). They generally showed minimal slopes in the [Zn^{2+}] range $10^{-10.5}$–$\sim 10^{-9.5}$ M ($\sim 10^{-8.5}$ M for clone BT6) with increasing slopes above and below this range. The curves were similar for all of the isolates and showed no apparent trends between neritic and oceanic algae within the Zn ion range of $10^{-12.2}$–$10^{-8.0}$M, characteristic of that for unpolluted marine waters (Bruland 1989). Cellular Zn : C ratios varied by no more than 3-fold among isolates within this range and by only 2-fold at the lowest [Zn^{2+}]. When cellular Zn : C ratios were multiplied by specific growth rates, the resultant specific uptake rates showed an even greater similarity among isolates with no more than a 2-fold variation over the entire experimental Zn ion range except at $10^{-8.0}$ M where there was a 3.5-fold variation (Fig. 4).

Uptake of Zn in the short-term kinetics studies with clone BT6 were dependent on both the Zn ion concentration in the immediate uptake medium and that in the medium in which the cells had been growing. Short-term uptake was markedly higher in cells previously grown at low [Zn^{2+}] (10^{-11} M) than in cells grown at high [Zn^{2+}] ($10^{-8.8}$ M) (Fig. 5). Cells generally showed linear uptake for the first 1–2 h and decreasing or increasing slopes thereafter. At [Zn^{2+}] $\geq 10^{-8.1}$ M, there was a small additional rapid uptake of Zn within the first 3 min, which probably reflected adsorption to sites on the cell surface.

Short-term cellular uptake rates were determined by linear regression for the initial 1–2-h linear uptake period. Resultant curves for Zn uptake rate vs. [Zn^{2+}] had sigmoidal shapes for both high- and low-Zn acclimated cells with a minimum in slope in the Zn ion range of 10^{-9}–10^{-8} M (Fig. 6). The rates were 30-fold higher for low-Zn than for high-Zn acclimated cells at the lowest Zn ion concentration in the uptake medium, but rates for the two groups of cells approached one another with increasing external Zn. At the highest level of Zn, uptake rates for the two groups differed by only 2.5-fold.

Discussion

Relationships between cellular Zn, cellular Zn uptake kinetics, and [Zn^{2+}]—The curves for steady state Zn uptake rate as a

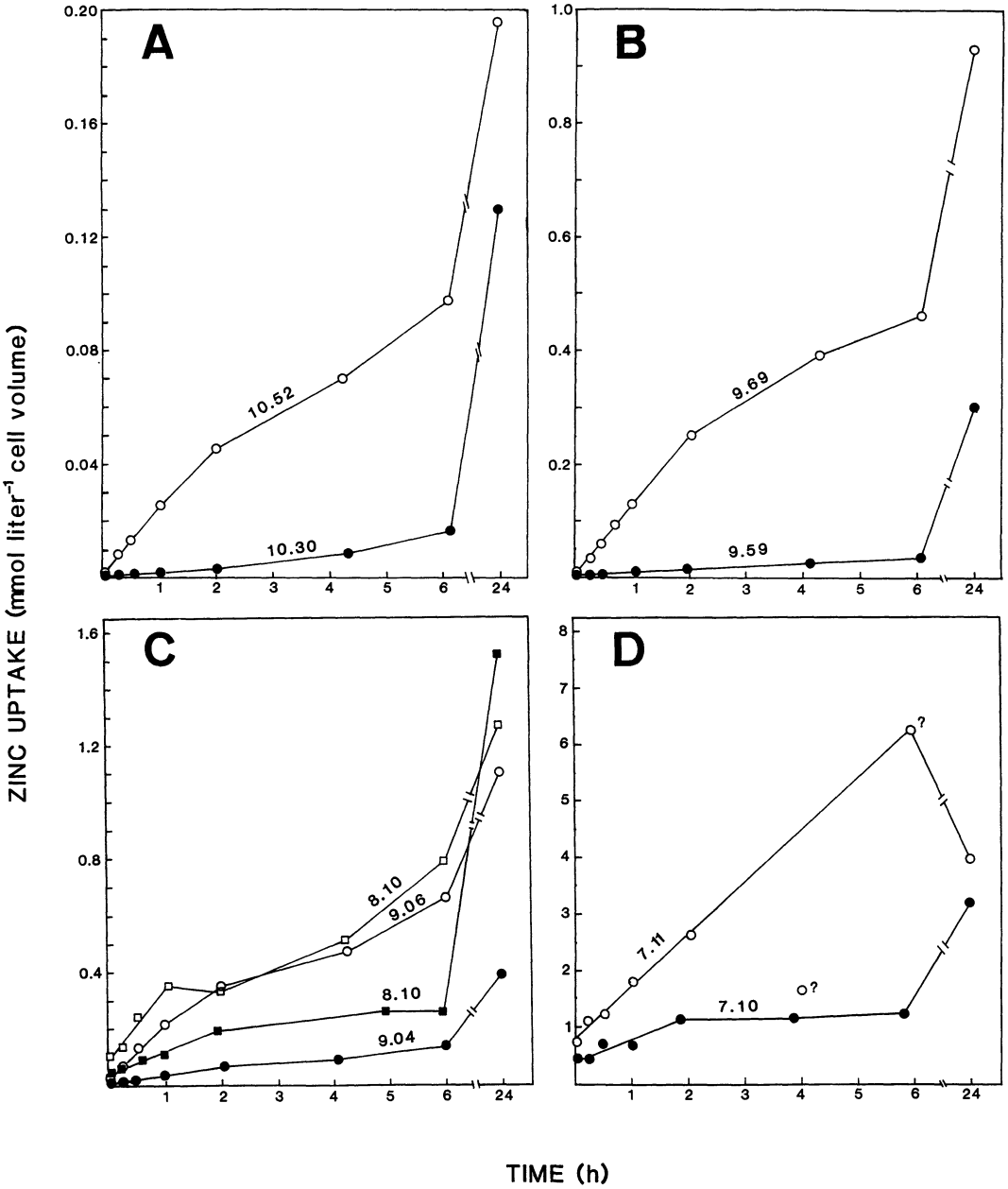

Fig. 5. Short-term uptake of Zn as a function of time for *Emiliania huxleyi* previously grown at high ($10^{-8.8}$ M—●, ■) and low ($10^{-11.0}$ M—○, □) [Zn^{2+}]. Uptake was measured at five separate Zn ion concentrations for each acclimated group of cells. Values for $-\log[Zn^{2+}]$ of the uptake medium are given above each curve. Note change in scale of *y*-axis among panels.

function of [Zn^{2+}] had sigmoidal shapes and showed an approximate proportionality between uptake rate and Zn ion concentrations at free ion concentrations $\leq 10^{-11.0}$ M, a minimum in slope at free ion concentrations between $10^{-10.5}$ and $\sim 10^{-9.5}$ M, and progressively increasing slopes above this range (Fig. 4). The relatively flat portions

of the curves at intermediate Zn ion concentrations appear to result from negative feedback regulation of cellular Zn uptake rate, as identified previously for the uptake of a number of other macro- and micronutrients, including nitrate (Gotham and Rhee 1981*b*), phosphate (Gotham and Rhee 1981*a*), Mn (Sunda and Huntsman 1985, 1986), and Fe (Harrison and Morel 1986).

For the above nutrients, uptake kinetics for cells grown at a single nutrient concentration followed the classical saturation (Michaelis-Menten) kinetics equation for facilitated or active uptake into the cell. For nutrient metals this equation can be written as

$$V = \frac{V_{max}[M]}{[M] + K_s} \quad (4)$$

where [M] is the concentration of either free metal ions or kinetically labile dissolved inorganic species (*see* Sunda 1991), V the uptake rate of metal, V_{max} the maximal uptake rate achieved when all of the membrane transport sites are bound to metal ions, and K_s the concentration of free metal ions, $[M^{n+}]$ (or dissolved inorganic metal species, [M']), at which half of the transport sites are bound and, therefore, at which V is half of V_{max}. For Fe and Mn, K_s is fixed, and V_{max} varies inversely with the metal ion concentration in the growth medium.

For these metals, as one decreases the metal concentration from values somewhat above to values below the half-saturation constant, there is a compensatory increase in V_{max} which allows cellular uptake rate, and therefore, cellular metal quota at constant growth rate, to remain relatively constant in spite of the decreasing saturation of the transport system. The capacity of the cells to increase V_{max} (e.g. by increasing the number of transport ligands in the outer membrane) is finite, and at metal ion concentrations below a critical level, V_{max} reaches a constant value. The transport rate then decreases essentially in proportion to the metal ion concentration because the transport system at this point is highly undersaturated.

Zn uptake by the cells appears to conform to the above negative feedback model with

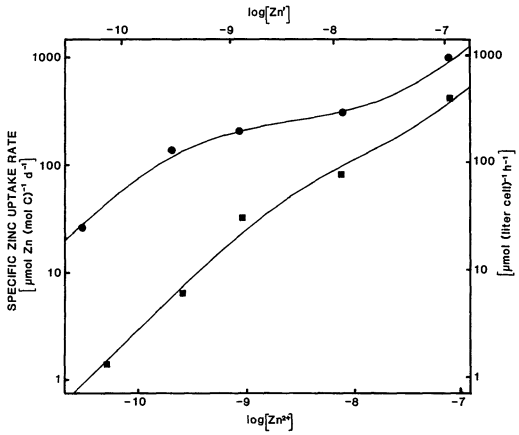

Fig 6. Initial linear Zn uptake rate as a function of $\log[Zn^{2+}]$ and log[Zn'] in the uptake medium for clone BT6 cells previously grown at Zn ion concentrations of $10^{-11.0}$ M (●) and $10^{-8.8}$ M (■). Curves fitted to the data are log-log plots of two-site transport models given by Eq. 5. Constants used to compute each curve are listed in Table 1.

two major exceptions. The first is that the short-term linear uptake kinetics, observed during the first 1–2 h of exposure to radiolabeled media, do not follow a simple saturation model for uptake by a single membrane transport site. Instead, the sigmoidal shape of the short-term transport kinetics curves in Fig. 6 indicates that Zn uptake involves at least two separate transport systems as represented mathematically by

$$V = \frac{V_{max}[Zn^{2+}]}{[Zn^{2+}] + K_s} + A[Zn^{2+}]. \quad (5)$$

The first term in the equation represents uptake by an inducible high-affinity site, and the second represents uptake by a low-affinity site for which $[Zn^{2+}] \ll K_s$. Under these undersaturated conditions, the uptake of Zn by the second site is essentially proportional to $[Zn^{2+}]$, with a proportionality constant, A, equal to V_{max}/K_s for that site.

The short-term Zn uptake rates during the first 1–2 h of exposure to ^{65}Zn could be fitted reasonably well to the above two-site transport model (Fig. 6). For cells of clone BT6 acclimated at a high $[Zn^{2+}]$ ($10^{-8.8}$ M), a reasonable fit was obtained for V_{max} equal to 109 μmol (mol C)$^{-1}$ d^{-1}, K_s equal to $10^{-8.4}$ M (expressed in terms of $[Zn^{2+}]$), and A equal

Table 1. Kinetic parameters for the two-site cellular Zn uptake model for clone BT6 (Eq. 5).

Acclimation log[Zn^{2+}]	V_{max} [μmol (mol C)$^{-1}$ d^{-1}]	log K_s*	A* [mol Zn (mol C)$^{-1}$ d^{-1} M^{-1}]
−8.8	109	8.4	3.5×10^3
−11.0	262	9.6	8.3×10^3

* Values for log K_s and A are expressed in terms of [Zn^{2+}]. To convert to values expressed in terms of dissolved [Zn'] requires that K_s be divided by 0.66 and A be multiplied by this same factor (*see Eq. 2*).

to 3.5×10^3 liters of medium (mol C)$^{-1}$ d^{-1}. Surprisingly, when uptake rate data for the low-Zn-acclimated cells were fitted to the model equation, the largest shift in the model parameters occurred in K_s, not V_{max} or A. The latter two parameters both increased by 2.4-fold, whereas there was a 16-fold decrease in K_s (Table 1). The large decrease in K_s, rather than an increase in V_{max}, in low-Zn-acclimated cells represents the second major difference between negative feedback regulation of transport observed previously for Mn and Fe and that described here for Zn.

The mechanism responsible for the large shift in K_s is not known. Possibilities include the induction at low Zn ion concentrations of a high-affinity Zn uptake system with fixed K_s, which is undetectable in cells acclimated at high Zn. Or there may be an actual shift in the K_s value for a single high-affinity uptake system due, for example, to allosteric shifts in molecular configuration at the transport binding site or to changes in localized charge on the membrane surface.

Despite the above uncertainties, it is clear that there is an increase in short-term uptake kinetics associated with decreases in external [Zn^{2+}] within the range $10^{-8.5}$–$10^{-10.5}$ M, which allows clone BT6 to maintain relatively constant cellular Zn uptake rates and, therefore, cellular Zn concentrations within that Zn ion range. At [Zn^{2+}] below this range, there is no further apparent change in the high-affinity transport system, and the steady state Zn uptake rates decrease proportionately with [Zn^{2+}] because the uptake system is highly undersaturated (Fig. 7). Above this range, the increase in slope for relationships between cellular Zn uptake rate and [Zn^{2+}] seems to be attributed to uptake by a second, low-affinity site, perhaps reflecting Zn leakage into the cell through the transport system of another metal ion (e.g. Mg^{2+}). Similar two-site negative feedback models probably also explain the sigmoidal shapes of curves for steady state Zn uptake rate vs. [Zn^{2+}] observed in the other algal species (Fig. 4).

In most cases the uptake rates in the short-term Zn experiments decreased with time after the initial 1–2-h linear uptake period. But for the high-Zn-acclimated cells transferred to the lowest [Zn^{2+}], the rate increased from a value of 1.3 μmol liter^{-1} h^{-1} during the first 2 h to 4.5 after 4–6 h (Fig. 5A). The increase in uptake rate that occurred after 2 h appears to be due to negative feedback increases in short-term transport rates as these cells began to acclimate to their new, much lower, [Zn^{2+}] environment. Likewise much of the decrease in transport rates that occurs after 1–2 h in cells transferred to higher Zn ion concentrations (the more typical case) is probably due to a negative-feedback down-shifting in transport rates. These time-dependent changes in short-term rates suggest that acclimation of Zn transport systems can occur within periods of several hours, similar to findings for feedback regulation of Mn transport in *T. pseudonana* and *T. oceanica* (Sunda and Huntsman 1986).

Relative Zn requirements of oceanic and coastal species—The oceanic species we studied were able to grow at maximal rates at much lower [Zn^{2+}] than coastal species, in agreement with previous studies with these and other coastal and oceanic isolates (Brand et al. 1983). Based on anodic stripping voltametric measurements, Bruland (1989) estimated [Zn^{2+}] in surface waters of the central North Pacific to be in the range of $1–2\times10^{-12}$ M. Such levels would substantially reduce the growth rates of the two coastal species, but would have little or no effect on the growth of the three oceanic isolates. These results support the hypothesis that low Zn availability has been an important factor in the ecology and evolution of oceanic species and that it has played a role in preventing coastal species from proliferating into oceanic waters. A similar ecological and evolutionary role has been ascribed to low oceanic Fe availability

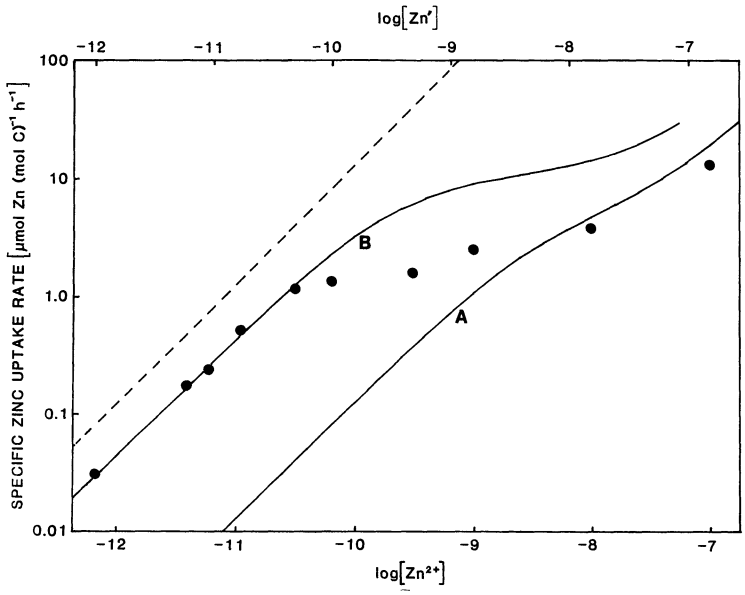

Fig. 7. Comparison of computed rates of steady state Zn uptake for clone BT6 (●) (*see Fig.4*) and the model curves for rate of short-term Zn uptake for cells acclimated to high (curve A) and low (curve B) $[Zn^{2+}]$ (*see Fig. 5*). At Zn ion concentrations above $\sim 10^{-8.5}$ M the steady state uptake of Zn by the cells approximately follows the short-term uptake curve for the high-Zn-acclimated cells (curve A). At Zn ion concentrations below $10^{-8.5}$ M, there is an increase in short-term uptake kinetics, involving a high-affinity system, which allows the cells to maintain relatively constant rates of steady state uptake, and therefore cellular Zn quotas, down to $[Zn^{2+}]$ of $10^{-10.5}$ M. Below this concentration, there is no further increase in short-term uptake kinetics, and the rates of steady state transport follow the short-term uptake curve for low-Zn-acclimated cells (curve B). Note that at $[Zn^{2+}] < 10^{-10.5}$ M, rates of cellular Zn uptake approach the limiting rate for diffusion of Zn' to the cell surface (dashed line of unity slope; *see Table 2*).

(Brand et al. 1983; Martin et al. 1989; Sunda et al. 1991).

The ability of oceanic species to grow well at substantially lower Zn ion concentrations than coastal species was due almost entirely to their much lower growth requirement for cellular Zn, rather than to any increased capability to take up Zn intracellularly. The same adaptation pattern has been found with regard to differences in the Fe requirement of *T. pseudonana* and *T. oceanica* (Sunda et al. 1991), one of the coastal-oceanic diatom pairs studied here. We had initially thought these results surprising since we had expected oceanic species to have adapted to the low levels of available Zn and Fe in their environments by evolving more effective transport systems as observed for other nutrients, such as nitrate (Carpenter and Guillard 1971) and Mn (Sunda and Huntsman 1986), that also occur at low oceanic concentrations.

Hudson and Morel (1990) recently examined the transport kinetics of the coastal species *T. weissflogii* and *Pleurochrysis carterae,* however, and found that their cellular Fe uptake rates approached the limits permitted by diffusion of dissolved inorganic Fe species to the cell surface and the kinetics of Fe ligand exchange at membrane uptake sites. They predicted that oceanic species could not evolve faster transport kinetics to adapt to the low Fe concentrations in their environment and, therefore, that these algae would have been forced to reduce their size or their cellular Fe requirement to survive.

Our present results indicate that a similar situation occurs with Zn. At the lowest experimental Zn ion concentration, the measured specific uptake rate for all isolates varied between 30 and 100% of the computed maximum rate for diffusion of labile inorganic Zn species to the cell surface (Table 2; Fig. 7). Thus, as with Fe, oceanic species

Table 2. Comparison between Zn uptake rates per cell and maximal diffusion rates of kinetically labile inorganic Zn species to the cell surface at [Zn'] of 1.02 pM.

	(A) Mean cell vol (μm^3)	(B) ESR (μm)	(C) Uptake rate (mol cell^{-1} h^{-1} × 10^{20})	(D) ρ (mol cell^{-1} h^{-1} × 10^{20})	(E) $\frac{C}{D} \times 100$ (%)
Thalassiosira pseudonona	40	2.1	1.74	5.9	29
Thalassiosira weissflogii	1,370	6.9	20	19.1	104
Thalassiosira oceanica	171	3.4	6.2	9.5	62
Emiliania huxleyi (BT6)	30	1.93	2.0	5.3	37
E. huxleyi (Al383)	49	2.3	2.5	6.4	39

* Maximal diffusion rate (ρ) computed from $\rho = 4\pi rD$ [Zn'] by assuming that the cells are about spherical in shape with a radius of r (Hudson and Morel 1990). D is the diffusion rate constant for Zn' at 20°C (6×10^{-6} cm^2 s^{-1}) and [Zn'] is the concentration of dissolved inorganic Zn species computed from Eq. 2. The equivalent spherical radius (column B) was computed from the mean cell volume measured by a Coulter counter using the relation between the radius of a sphere and its volume.

seem to have been unable to evolve more effective Zn transport systems because the transport kinetics of coastal species already approach the physical limits permitted by diffusion. An onset of diffusion limitation also would explain why the negative feedback regulation of cellular Zn uptake, discussed earlier, does not persist below [Zn^{2+}] of $10^{-10.5}$ M (Fig. 7).

Although oceanic species have been forced to reduce their cellular growth requirements for Zn, Fe, and other trace metal nutrients such as Mn (Sunda and Huntsman 1986), the mechanisms by which they do so are unknown. Possibilities include more efficient use of internal metal micronutrient pools, or the replacement of enzymes containing scarce metals with ones containing more available metals, or having no metallic cofactors at all (Sunda 1991). With regard to the second of these possibilities, it is now known that Cd can be substituted for Zn in fulfilling the Zn nutritional requirements of *T. weissflogii* (Price and Morel 1990). The ecological importance of this replacement, however, may be limited in the ocean due to the much lower concentration of Cd relative to Zn. For example, in surface seawater from the central North Pacific, total Zn occurs at a concentration of ~70 pM whereas Cd is present at only 1.4 pM (Bruland 1980).

Regulation of oceanic Zn concentrations by phytoplankton uptake and regeneration—The relationships between cellular Zn : C ratios and [Zn^{2+}] were compared with the relative depth-dependent changes in Zn and major nutrient concentrations and Zn speciation to determine if uptake by phytoplankton can account for observed marine Zn distributional patterns, as in the classical Redfield model for biological regulation of major nutrients (Redfield et al. 1963). Redfield et al. found that C, N, and P occur in approximately constant molar ratios of 106 : 16 : 1 in plankton and demonstrated that the relative depth-dependent changes in concentrations of these elements in the ocean generally equal these ratios. These observations provided strong evidence that the concentrations of the major nutrients in seawater are controlled by planktonic uptake and regeneration.

In applying the Redfield model to Zn, we must be aware of differences in the patterns of phytoplankton uptake of major nutrients and Zn. Unlike the major nutrients, whose ratios to each other in marine plankton are more or less the same irrespective of their concentrations in seawater, phytoplankton Zn : C ratios increase with increasing external Zn. Consequently, phytoplankton should remove Zn from seawater in increasing amounts relative to N, C, and P with increasing Zn ion concentration. Thus, if phytoplankton are primarily responsible for Zn removal from seawater, the relationship between Zn and major nutrient concentrations should be curvilinear, with increasing slopes at increasing concentrations.

The relationships between dissolved Zn and PO_4 in the nutriclines (0–800 m) of three stations in the eastern North Pacific, based on data of Bruland (1980), have this characteristic (Fig. 8). If these curves do, in fact, reflect the relative removal of Zn and PO_4

by phytoplankton, then the slopes (dZn/dPO_4) should reflect the relative amounts of Zn and PO_4 in phytoplankton cells at the ambient $[Zn^{2+}]$ in the water at the time these elements were removed. We tested this hypothesis by computing the slopes for the relative changes in Zn and PO_4 concentrations ($\Delta Zn/\Delta PO_4$) for water from adjacent depths within the nutriclines of Bruland's vertical profiles (*see Fig. 8*). The resultant Zn : PO_4 ratios were converted to Zn : C ratios using the Redfield C : P ratio for plankton of 106 : 1. The Zn : C ratios were then plotted as a function of the computed Zn ion concentration at the mean Zn concentration for the depth interval. Values of $[Zn^{2+}]$ were computed from the speciation model described in the methods section for Zn complexation in central North Pacific seawater based on data of Bruland (1989).

The modeled relationship between Zn : C ratios and $[Zn^{2+}]$ determined from the analysis of the Zn and PO_4 distributions within the nutricline agreed well with relationships between cellular Zn : C and $[Zn^{2+}]$ measured in our phytoplankton cultures (Fig. 9). Thus, as in the Redfield model for major nutrients, this agreement provides strong evidence that uptake of Zn by phytoplankton is primarily responsible for its removal from surface seawater and directly accounts for distributional patterns in Zn concentrations in the nutricline.

As mentioned above, a major difference between the Redfield model for Zn and that for major nutrients is the decrease in Zn uptake by phytoplankton with decreasing Zn ion concentrations. This factor does not affect the model in terms of cellular removal of Zn from seawater, but it does have an effect with regard to Zn regeneration because, as a result of particle sinking, such regeneration will tend to occur in deeper water with higher Zn : major nutrient ratios than the surface water in which uptake occurred. Such an effect will tend to dampen relative changes in $\Delta Zn/\Delta PO_4$ observed with depth and may explain why Zn : C ratios determined from the model show a somewhat smaller variation over the environmental Zn ion range than do the measured cellular Zn : C ratios in phytoplankton cells (Fig. 9).

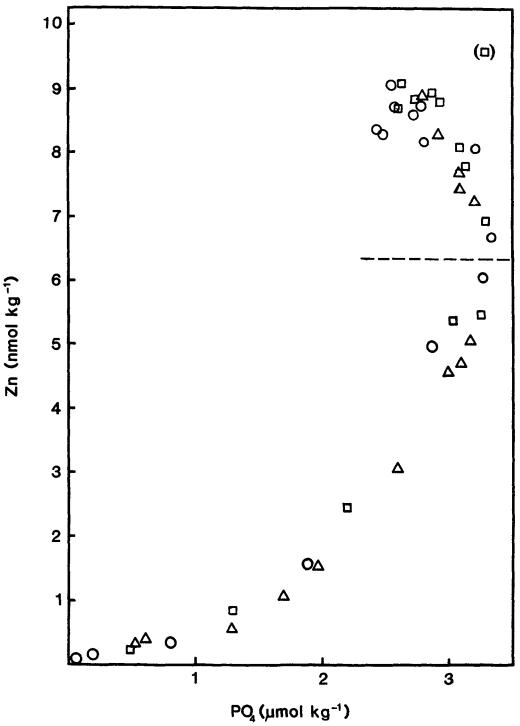

Fig. 8. Relationship between Zn and PO_4 concentrations at three stations in the eastern North Pacific (○—H-77, 32°41.0′N, 144°59.5′W; □—C-I, 37°0.0′N, 124°12.0′W; and △—C-II, 36°52.0′N, 122°53.0′W). Points below the dashed line give data within the nutricline (0–800 m), those above give data from greater depths (950–4,900 m). (Data from Bruland 1980.)

Redfield et al. (1963), however, pointed out that high nutrient concentrations at depth not only reflect remineralization of sinking biogenic particles, but also the marked lateral differences in surface concentrations between nutrient-impoverished tropical and temperate waters and nutrient-rich polar seas as well as the subduction and subsequent lateral advection of dense polar water along isopycnal surfaces. Through this mechanism, biologically driven changes in macro- and micronutrient concentrations that occur laterally in surface waters can be transposed directly into vertical variations in concentrations.

Below the PO_4 maximum, which occurs at ~800 m at the three North Pacific stations, the Zn concentration continues to increase with depth while that of PO_4 decreases, leading to a negative correlation between

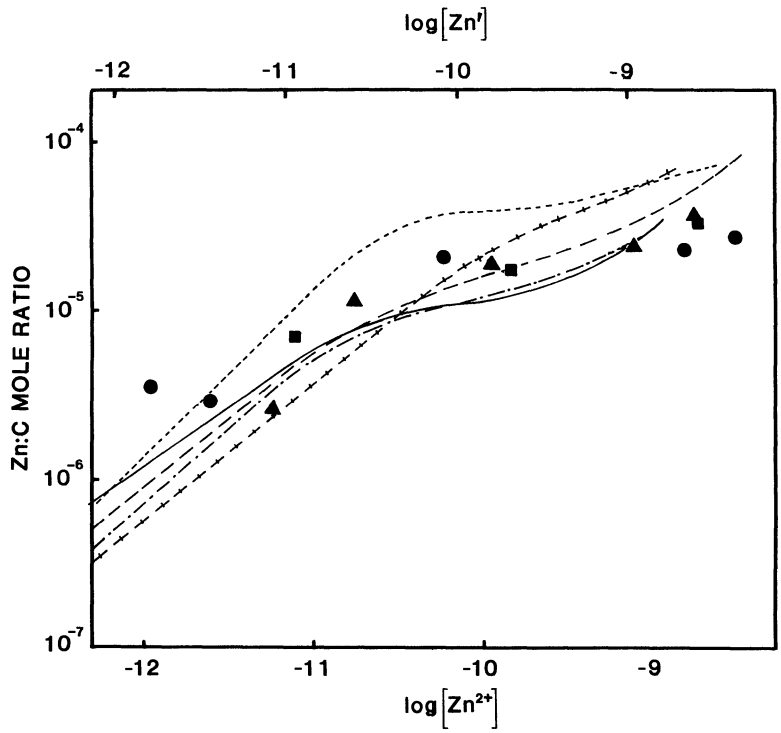

Fig. 9. Computed relationships between the molar ratio of Zn : C and log[Zn^{2+}] determined from dissolved Zn vs. PO_4 relationships in the nutriclines of three stations in the eastern North Pacific (*see Fig. 8*). Symbols indicate values computed for stations H-77 (●), C-I (■), and C-II (▲). Lines give relationships between cellular Zn : C ratios and log[Zn^{2+}] measured in algal cultures as plotted in Fig. 3.

Zn and PO_4 (Fig. 8). A similar situation occurs at these stations with Ni and Si, which both increase with increasing PO_4 concentrations at depths above the PO_4 maximum, but are negatively correlated with PO_4 at greater depths. This difference in correlative behavior above and below the nutrient maximum suggests that processes besides biogenic scavenging and remineralization influence the distributions of many macro- and micronutrient elements in the deep sea, which in the North Pacific includes water with ages of up to 1,000 yr since it last resided at the surface. Such deep-sea processes might include hydrothermal inputs of Zn, Ni, and Si (Edmond et al. 1979; Von Damm 1990), PO_4 coprecipitation with hydrothermally produced Fe oxides (Feely et al. 1990), and differential release into overlying waters of nutrient elements regenerated from biogenic matter in deep-sea sediments (e.g. release of silica and relative retention of Fe and PO_4).

Conclusions

Results of our investigation support the general hypothesis of mutual interactions between Zn concentrations in seawater and marine phytoplankton communities. Data presented here along with previous data provide evidence that Zn could be an important factor in controlling algal species composition by preventing proliferation of coastal species into low-Zn oceanic environments. There is no evidence, however, for Zn limitation of growth of oceanic or coastal species in their own respective habitats. The effect of Zn on marine algal communities appears to be reciprocal. Our results provide evidence that Zn concentrations within the nutricline are regulated by algal uptake and regeneration processes

similar to those that regulate major nutrient concentrations.

References

ANDERSON, M. A., F. M. M. MOREL, AND R. R. L. GUILLARD. 1978. Growth limitation of a coastal diatom by low zinc ion activity. Nature **276:** 70–71.

BRAND, L. E., W. G. SUNDA, AND R. R. L. GUILLARD. 1983. Limitation of marine phytoplankton reproductive rates by zinc, manganese, and iron. Limnol. Oceanogr. **28:** 1182–1198.

———, ———, AND ———. 1986. Reduction of marine phytoplankton reproduction rates by copper and cadmium. J. Exp. Mar. Biol. Ecol. **96:** 225–250.

BRULAND, K. W. 1980. Oceanographic distributions of cadmium, zinc, nickel and copper in the North Pacific. Earth Planet. Sci. Lett. **47:** 176–198.

———. 1989. Complexation of zinc by natural organic ligands in the central North Pacific. Limnol. Oceanogr. **34:** 269–285.

———, AND R. P. FRANKS. 1983. Mn, Ni, Cu, Zn, and Cd in the western North Atlantic, p. 395–414. *In* Trace metals in sea water. NATO Conf. Ser. 4: Mar. Sci. V. 9. Plenum.

BYRNE, R. H., L. R. KUMP, AND K. J. CANTRELL. 1988. The influence of temperature and pH on trace metal speciation in seawater. Mar. Chem. **25:** 163–181.

CARPENTER, E. J., AND R. R. L. GUILLARD. 1971. Intraspecific differences in nitrate half-saturation constants for three species of marine phytoplankton. Ecology **52:** 183–185.

DONAT, J. R., AND K. W. BRULAND. 1990. A comparison of two voltammetric methods for determining zinc speciation in northeast Pacific Ocean waters. Mar. Chem. **28:** 301–323.

EDMOND, J. M., AND OTHERS. 1979. Ridgecrest hydrothermal activity and the balances of major and minor elements in the oceans: The Galapagos data. Earth Planet. Sci. Lett. **46:** 1–18.

EVANS, D. W. 1977. Exchange of manganese, iron, copper, and zinc between dissolved and particulate forms in the Newport River estuary, North Carolina. Ph.D. thesis, Oregon State Univ. 218 p.

FEELY, R. A., AND OTHERS. 1990. The effect of hydrothermal processes on midwater phosphorus distributions in the northeast Pacific. Earth Planet. Sci. Lett. **96:** 305–318.

GOTHAM, I. J., AND G-Y. RHEE. 1981*a*. Comparative kinetic studies of phosphate limited growth and phosphate uptake in phytoplankton in continuous culture. J. Phycol. **17:** 257–265.

———, AND ———. 1981*b*. Comparative kinetic studies of nitrate limited growth and nitrate uptake in phytoplankton in continuous culture. J. Phycol. **17:** 309–314.

GUILLARD, R. R. L., AND J. H. RYTHER. 1962. Studies of marine planktonic diatoms. 1. *Cyclotella nana* (Hustedt) and *Detonula confervacea* (Cleve) Gran. Can. J. Microbiol. **8:** 229–239.

HARRISON, G. I., AND F. M. M. MOREL. 1983. Antagonism between cadmium and iron in the marine diatom *Thalassiosira weissflogii*. J. Phycol. **19:** 495–507.

———, AND ———. 1986. Response of the marine diatom *Thalassiosira weissflogii* to iron stress. Limnol. Oceanogr. **31:** 989–997.

HUDSON, R. J. M., AND F. M. M. MOREL. 1990. Iron transport in marine phytoplankton: Kinetics of cellular and medium coordination reactions. Limnol. Oceanogr. **35:** 1002–1020.

MARTELL, A. E., AND R. M. SMITH. 1974. Critical stability constants. V. 1. Amino acids. Plenum.

MARTIN, J. H., AND R. M. GORDON. 1988. Northeast Pacific iron distributions in relation to phytoplankton productivity. Deep-Sea Res. **35:** 177–196.

———, ———, S. FITZWATER, AND W. W. BROENKOW. 1989. VERTEX: Phytoplankton/iron studies in the Gulf of Alaska. Deep-Sea Res. **36:** 649–680.

MOREL, F. M. M., AND R. J. M. HUDSON. 1984. The geobiological cycle of trace elements in aquatic systems: Redfield revisited, p. 251–281. *In* W. Stumm [ed.], Chemical processes in lakes. Wiley.

PRICE, N. M., AND F. M. M. MOREL. 1990. Cadmium and cobalt substitution for zinc in a marine diatom. Nature **344:** 658–660.

REDFIELD, A. C., B. H. KETCHUM, AND F. A. RICHARDS. 1963. The influence of organisms on the composition of seawater, p. 26–77. *In* M. N. Hill [ed.], The sea. V. 2. Wiley.

SUNDA, W. G. 1984. Measurement of manganese, zinc, and cadmium complexation in seawater using Chelex ion exchange equilibria. Mar. Chem. **14:** 365–378.

———. 1991. Trace metal interactions with marine phytoplankton. Biol. Oceanogr. **6:** 411–442.

———, AND R. R. L. GUILLARD. 1976. The relationship between cupric ion activity and the toxicity of copper to phytoplankton. J. Mar. Res. **34:** 511–529.

———, AND A. K. HANSON. 1987. Measurement of free cupric ion concentration in seawater by a ligand competition technique involving copper sorption onto C_{18} SEP-PAK cartridges. Limnol. Oceanogr. **32:** 537–551.

———, AND S. A. HUNTSMAN. 1983. Effect of competitive interactions between manganese and copper on cellular manganese and growth in estuarine and oceanic species of the diatom *Thalassiosira*. Limnol. Oceanogr. **28:** 924–934.

———, AND ———. 1985. Regulation of cellular manganese and manganese transport rates in the unicellular alga *Chlamydomonas*. Limnol. Oceanogr. **30:** 71–80.

———, AND ———. 1986. Relationships among growth rate, cellular manganese concentrations, and manganese transport kinetics in estuarine and oceanic species of the diatom *Thalassiosira*. J. Phycol. **22:** 259–270.

———, D. G. SWIFT, AND S. A. HUNTSMAN. 1991.

Low iron requirement for growth in oceanic phytoplankton. Nature **351:** 55–57.

———, P. A. TESTER, AND S. A. HUNTSMAN. 1990. Toxicity of trace metals to *Acartia tonsa* in the Elizabeth River and southern Chesapeake Bay. Estuarine Coastal Shelf Sci. **30:** 207–221.

VON DAMM, K. L. 1990. Seafloor hydrothermal activity: Black smoker chemistry and chimneys. Annu. Rev. Earth Planet. Sci. **18:** 173–204.

Submitted: 25 June 1991
Accepted: 27 June 1991
Revised: 25 November 1991